

Superconducting states for semi-Dirac fermions at zero and finite magnetic fields

Bruno Uchoa* and Kangjun Seo

Department of Physics and Astronomy, University of Oklahoma, Norman, Oklahoma 73069, USA

(Received 3 June 2017; published 15 December 2017)

We address the superconducting singlet state of anisotropic Dirac fermions that disperse linearly in one direction and parabolically in the other. For systems that have uniaxial anisotropy, we show that the electromagnetic response to an external magnetic flux is extremely anisotropic near the quantum critical point of the superconducting order. In the quantum critical regime and above a critical magnetic field, we show that the superconductor may form an exotic *smectic* state, with a stripe pattern of flux domains.

DOI: [10.1103/PhysRevB.96.220503](https://doi.org/10.1103/PhysRevB.96.220503)

Introduction. Semi-Dirac metals form a class of two-dimensional (2D) systems with chiral quasiparticles that disperse linearly in one direction and quadratically in a different direction [1]. In the presence of spin-orbit coupling, the zero energy crossings of the Dirac cones remain protected by space group symmetries of the crystal [2] and may have a nonzero Chern number [3,4]. Examples of semi-Dirac metals include a variety of systems, including VO₂/TiO₂ heterostructures [3,5], and strained crystals such as graphene and black phosphorus, which can undergo a topological phase transition towards a semi-Dirac phase [6,7]. Semi-Dirac cones have been experimentally realized on the top layer of black phosphorus under electric field effects, which tune the system from a trivial band gap insulator to a band inverted system [8].

In this Rapid Communication, we explore the properties of *s*-wave singlet states for semi-Dirac fermions in the vicinity of a quantum critical point (QCP). We show that semi-Dirac fermion superconductors have an exotic electromagnetic response to an applied magnetic flux. Due to the anisotropy of the quasiparticles, the stiffness of the order parameter to the penetration of a magnetic flux can be highly anisotropic near the QCP. In that regime, we show that semi-Dirac metals with uniaxial anisotropy can effectively behave as type-I superconductors along one direction, and as type-II superconductors in the other. As a result, instead of vortices, the system may form a smectic state with stripes of superconducting domains intercalated by thin normal strips of magnetic flux [9].

Hamiltonian. For concreteness, we start from a two-orbital model on a square lattice,

$$\mathcal{H}_0(\mathbf{k}) \equiv \mathbf{g}(\mathbf{k}) \cdot \vec{\sigma}, \quad (1)$$

where $\mathbf{g} = (g_x, g_y, g_z)$ is a vector with components $g_x(\mathbf{k}) = 4t'(\cos k_x - \cos k_y)^2$, $g_y(\mathbf{k}) = 0$, and $g_z(\mathbf{k}) = 2t(\cos k_x + \cos k_y)$, t and t' are effective hopping parameters, k is the momentum with respect to the center of the square Brillouin zone, and σ_x and σ_z are Pauli matrices in the orbital space [1]. The low-energy Hamiltonian is described by semi-Dirac fermions around four nodal points $\mathbf{k}_0 = (\pm\frac{1}{2}, \pm\frac{1}{2})\pi$, with

$$\mathcal{H}_{0,\alpha}^{(+)}(\mathbf{p}) = \frac{p_x^2}{2m}\sigma_x - \alpha v p_y \sigma_z \equiv \mathbf{h}_{+,\alpha}(\mathbf{p}) \cdot \vec{\sigma}, \quad (2)$$

describing the pair of nodes at $\mathbf{k}_0 = \alpha(\frac{1}{2}, \frac{1}{2})\pi$ ($\alpha = \pm$), where \mathbf{p} is the momentum away from the nodes (we set $\hbar \rightarrow 1$),

with p_x and p_y as momentum coordinates along the two diagonal directions $(1, \bar{1})$ and $(1, 1)$, respectively. m is the mass of the quasiparticles that disperse quadratically with momentum p_x along one direction and v gives the Fermi velocity of the quasiparticles that disperse linearly along the perpendicular direction. The other two nodes at $\mathbf{k}_0 = \alpha(\frac{1}{2}, -\frac{1}{2})\pi$ are described by the low-energy Hamiltonian

$$\mathcal{H}_{0,\alpha}^{(-)}(\mathbf{p}) = -\alpha v p_x \sigma_x + \frac{p_y^2}{2m}\sigma_z \equiv \mathbf{h}_{-,\alpha}(\mathbf{p}) \cdot \vec{\sigma}. \quad (3)$$

In both sets of pairs, opposite nodal points are related by time-reversal symmetry (TRS).

The Bogoliubov–de Gennes Hamiltonian for Eq. (1) is

$$\mathcal{H}_{\text{BdG}}(\mathbf{k}) = \begin{pmatrix} \mathcal{H}_0(\mathbf{k}) & \hat{\Delta} \\ \hat{\Delta} & -T\mathcal{H}_0(\mathbf{k})T^{-1} \end{pmatrix}, \quad (4)$$

where the 2×2 matrix $\hat{\Delta}$ gives superconducting order parameter matrix elements in the orbital space and $T\mathcal{H}_0(\mathbf{k})T^{-1} = \mathcal{H}_0(\mathbf{k})$ is the TRS operation of the Hamiltonian.

In the singlet state, there are two possible pairing channels. The first one is the intraorbital pairing state, with pairing matrix elements $\hat{\Delta} = \Delta\sigma_0$, which result in a fully gapped low-energy spectrum

$$\pm E_{\mathbf{p}} = \pm\sqrt{h^2(\mathbf{p}) + \Delta^2}, \quad (5)$$

with $h(\mathbf{p}) = |\mathbf{h}(\mathbf{p})|$ (the valley indices are omitted). The second channel is the interorbital pairing state, $\hat{\Delta} = \Delta\sigma_x$, which leads to gapless superconductivity, $\pm E_{\mathbf{p},s} = \pm\sqrt{h_x^2(\mathbf{p}) + [h_z(\mathbf{p}) + s\Delta]^2}$, with $s = \pm$ indexing two additional branches, shown in Fig. 1(b). For a given attractive interaction, the fully gapped state lowers the free energy of the system more than the gapless one by pushing the energy states down towards the bottom of the band, as shown in Fig. 1(a). In this Rapid Communication, we will focus on the dominant instability and address the thermodynamic and electromagnetic properties of the fully gapped state.

Critical behavior. The free energy of the superconducting state is $F(T) = \Delta^2/g - T \sum_{\mathbf{k},\gamma} \log\{2 + 2 \cosh(\gamma E_{\mathbf{k}}/T)\}$, with $\gamma = \pm$ indexing the particle and hole branches of the spectrum, respectively, T is the temperature, and $g > 0$ is the effective attractive interaction that leads to the formation of Cooper pairs. At the mean field level, minimization of the free energy with respect to Δ (assumed to be real) gives the standard BCS equation of state $g^{-1} = \sum_{\mathbf{q}} \tanh(\frac{1}{2T} E_{\mathbf{q}})/2E_{\mathbf{q}}$. Using the parametrization where $h_x(\mathbf{p}) = p_x^2/2m = h \cos \theta$ and

*uchoa@ou.edu

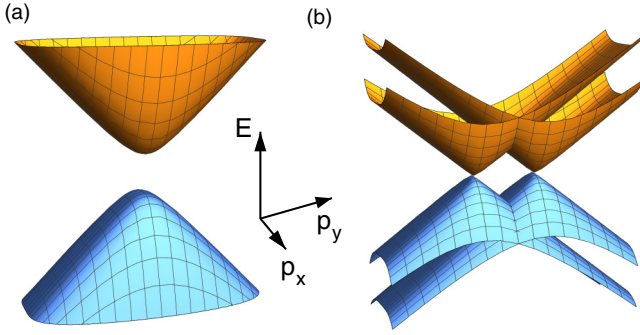


FIG. 1. Energy spectrum of the superconducting singlet states of semi-Dirac fermions. (a) Intraorbital pairing state, which is fully gapped around each nodal point. (b) Interorbital state, where the nodes split and remain gapless. The gapped state is dominant.

$h_z(\mathbf{p}) = vp_y = h \sin \theta$, with $\theta \in [-\frac{\pi}{2}, \frac{\pi}{2}]$, the density of states can be written in terms of the Jacobian of the transformation $(p_x, p_y) \rightarrow (h, \theta)$ [10],

$$\rho(h, \theta) = \frac{N_0 \sqrt{2mh}}{8\pi^2 v \cos \theta}. \quad (6)$$

Integration in θ gives the actual density of states, $\rho(h) = 2 \int_{-\pi/2}^{\pi/2} d\theta \rho(h, \theta) = \rho_0 \sqrt{h}$, where $\rho_0 = \sqrt{m} N_0 K(\frac{1}{2}) / (\pi^2 v)$, with $K(\frac{1}{2}) \approx 1.85$ an elliptic function and N_0 is the node degeneracy.

At zero temperature and half filling, the phase transition is quantum critical due to the vanishing density of states (DOS) at the nodal point [11–13]. Near the QCP, the mean-field zero-temperature gap scales with the coupling as

$$\Delta(0, g) = \frac{1}{(c_1 \rho_0)^2} \left(\frac{1}{g_c} - \frac{1}{g} \right)^2 \theta (g - g_c), \quad (7)$$

where $c_1 = \Gamma^2(\frac{3}{4})/\sqrt{\pi} \approx 0.85$, with $\Gamma(x)$ a gamma function, and $g_c = 1/(\sqrt{\Lambda} \rho_0)$ is the critical coupling defined in terms of the effective energy bandwidth Λ . In the gapless state, the critical coupling is $g'_c = 3/(\sqrt{2\Lambda} \rho_0) > g_c$, and hence the gapped instability clearly prevails. In the two-band model (1) where $m^{-1} = 16t'$, $v = 2\sqrt{2}t$, and $\Lambda \sim 2t$, then $g_c/t = 8\pi^2/[N_0 K(\frac{1}{2})]\sqrt{t'/t}$. In the limit where $t'/t \ll 1$, the critical coupling can be small enough to allow the QCP physics to be accessed experimentally. In general, since $g_c \propto v/\sqrt{m}$ scales with the velocity and mass of the quasiparticles, the critical coupling can be further lowered with strain effects [14].

The mean-field critical temperature is given by $T_c(g) \approx c_1^2 \Delta(0, g)$, as shown in Fig. 2. In the critical regime,

$$\Delta(T \approx T_c, g) \approx 2.02 \Delta(0, g) \sqrt{\frac{T_c}{T} - 1}. \quad (8)$$

The specific heat at fixed volume is defined as $C_V = -T d^2 F / dT^2$. At the phase transition, the specific heat jump normalized by the specific heat in the normal side of the transition is universal, $\delta C_V \approx 0.71$ [15]. In the case of Dirac fermions in 2D (graphene), $\delta C_V \approx 0.35$ [16], while in the Fermi liquid case $\delta C_V \approx 1.43$ [17].

Supercurrent. To calculate the Meissner response to an external magnetic flux, we include a vector potential \mathbf{A} in

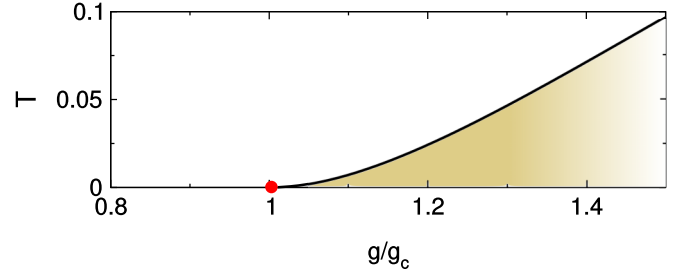


FIG. 2. Phase diagram of temperature (in units of the cutoff Λ) vs coupling for the fully gapped state in the vicinity of the QCP at $g = g_c$. The order parameter scales as $\Delta \propto (1 - g_c/g)^\beta$ near the QCP, with $\beta = 2$ in mean field.

Hamiltonian (4) in the Coulomb gauge, explicitly breaking TRS, $T \mathcal{H}_0(\mathbf{k} - \frac{e}{c} \mathbf{A}) T^{-1} = \mathcal{H}_0(\mathbf{k} + \frac{e}{c} \mathbf{A})$. When the Fermi level is at the neutrality point, the energy spectrum can be calculated analytically,

$$E_{\mathbf{k}, s}(\mathbf{A}) = \sqrt{g_D^2 + g_\xi^2 + \Delta^2 + 2s \sqrt{(g_D \cdot g_\xi)^2 + g_\xi^2 \Delta^2}}, \quad (9)$$

with $s = \pm$, and $g_{D, \xi} = |\mathbf{g}_{D, \xi}|$, with $\mathbf{g}_{D, \xi}(\mathbf{k}) = \frac{1}{2} \sum_{s=\pm} s^q \mathbf{g}(\mathbf{k} - s \frac{e}{c} \mathbf{A})$, where $q = 0, 1$ describe the symmetric (D) and antisymmetric (ξ) combinations in the vector potential, respectively.

The calculation of the supercurrent from Eqs. (1) and (4) can be done in a very general way for any arbitrary vector $\mathbf{g} = (g_x, g_y, g_z)$ defined in terms of generic functions of momenta $g_i(\mathbf{k})$, $i = x, y, z$, provided TRS is preserved at zero field. From the minimal coupling between currents and electromagnetic fields, $\mathcal{H}_i = \frac{1}{c} \mathbf{j} \cdot \mathbf{A}$, the current operator is $\mathbf{j} = c \partial \mathcal{H}_{\text{BdG}} / \partial \mathbf{A}$. The supercurrent in the London limit is $\langle \mathbf{j} \rangle = -c \text{tr} \frac{1}{\beta} \sum_{i\omega, \mathbf{k} \in \text{BZ}} [\partial_{\mathbf{A}} \mathcal{H}_{\text{BdG}}(\mathbf{k}, \mathbf{A})] \hat{G}_{\mathbf{k}}(i\omega)$, where $\hat{G}_{\mathbf{k}}(i\omega) = [i\omega - \hat{\mathcal{H}}_{\text{BdG}}(\mathbf{k}, \mathbf{A})]^{-1}$ is the Green's function.

In leading order in the vector potential, the diamagnetic response in the Coulomb gauge is given by $\langle j_i \rangle = K_{ij} A_j$, where K_{ij} is the London kernel. For anisotropic superconductors that preserve inversion symmetry, the kernel has the form $K_{ij} = (\delta_{ij} - \hat{k}_i \hat{k}_j) Q_j$, with \hat{k} a unitary vector [18]. The off-diagonal components of the kernel result from phase modes [19], which ensure that the static continuity equation $\mathbf{k} \cdot \langle \mathbf{j} \rangle = 0$ is satisfied in the Coulomb gauge. Alternatively, we can simply fix the gauge in such a way that $\langle j_i \rangle = Q_i A_i$. After a proper regularization of the deep energy states at the bottom of the band [20], which is done by imposing periodic boundary conditions at the edge of the Brillouin zone [18], the London kernel per node is

$$Q_i = \frac{e^2}{\hbar^2 c} \Delta^2 \sum_{\mathbf{p}} \partial_{E_{\mathbf{p}}} \left[\frac{\tanh(E_{\mathbf{p}}/2T)}{E_{\mathbf{p}}} \right] \frac{[\partial_{p_i} \mathbf{h}(\mathbf{p})]^2}{E_{\mathbf{p}}}, \quad (10)$$

restoring \hbar . Although $\langle j_i \rangle$ is calculated in a fixed gauge, gauge invariance is restored by screening effects [21], which preserve the transversality condition of the supercurrent, $\mathbf{k} \cdot \langle \mathbf{j} \rangle = 0$, irrespective of the gauge choice [22].

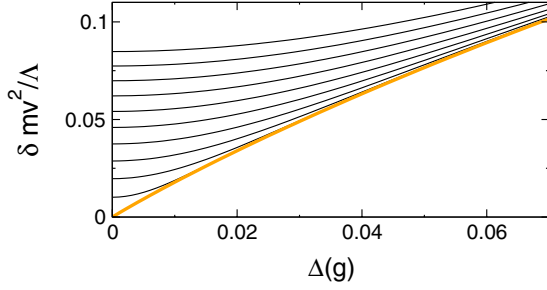


FIG. 3. Anisotropy $\delta \equiv Q_x/Q_y$ per node times mv^2/Λ vs coupling $\Delta(T_0, g)$ (in Λ cutoff units) for different temperatures T_0 . T_0/Λ ranges from zero (orange line) to 0.025 in 0.0025 steps. At $T_0 = 0$, δ scales to zero at the QCP. In that limit, the Meissner response becomes quasi-one-dimensional.

In the semi-Dirac case, the supercurrent due to each node is anisotropic, as expected, with

$$\langle j_x \rangle(T) = \frac{e^2}{\hbar^2 c} \frac{\Gamma^2(\frac{3}{4})}{\pi^{5/2}} \Theta_1(T) \frac{1}{\sqrt{mv}} A_x, \quad (11)$$

and

$$\langle j_y \rangle(T) = \frac{e^2}{\hbar^2 c} \frac{K(\frac{1}{2})}{2\pi^2} \Theta_0(T) \sqrt{mv} A_y, \quad (12)$$

where $\Theta_n(T) = \Delta^2 \int_0^\infty dh h^n \sqrt{h} \frac{1}{E} \partial_E [\tanh(\frac{E}{2T})/E]$, with $E = \sqrt{\hbar^2 + \Delta^2}$. This integral can be analytically calculated in the zero-temperature limit and close to the critical temperature,

$$\Theta_0(T) = - \begin{cases} \frac{1}{\sqrt{\pi}} \Gamma^2(\frac{3}{4}) \sqrt{\Delta}, & \text{for } T = 0, \\ a_0 \frac{\Delta^2(T)}{(2T)^{\frac{3}{2}}}, & \text{for } T \approx T_c, \end{cases} \quad (13)$$

where $a_0 = \int_0^\infty dx x^{-\frac{3}{2}} [x^{-1} \tanh x - \text{sech}^2 x] \approx 0.79$, and

$$\Theta_1(T) = - \begin{cases} \frac{1}{4\sqrt{\pi}} \Gamma^2(\frac{1}{4}) \Delta^{\frac{3}{2}}, & \text{for } T = 0, \\ a_1 \frac{\Delta^2(T)}{\sqrt{2T}}, & \text{for } T \approx T_c, \end{cases} \quad (14)$$

with $a_1 = \frac{1}{2} \int_0^\infty dx x^{-\frac{3}{2}} \tanh x \approx 1.91$.

Near the critical temperature, the kernel anisotropy $\delta(T, g) \equiv Q_x/Q_y \propto T_c(g)/(mv^2)$ scales linearly with T_c and vanishes at the QCP. In the zero-temperature limit, $\delta(0, g) \sim \Delta(g)/(mv^2)$, and hence the anisotropy $\delta(0, g) \rightarrow 0$ linearly with the gap as one approaches the QCP at $g = g_c$ (orange line in Fig. 3). In that limit, the system is extremely anisotropic [23], with relativistic quasiparticles carrying a supercurrent along the direction of linear dispersion. In Fig. 3, we show the plot of the anisotropy per node δ versus the gap $\Delta(T_0, g)$ for fixed temperatures T_0 . When $\Delta \lesssim T_0$, the kernel Q_i has a crossover from the anomalous zero-temperature scaling regime, $Q_x \propto \Delta^{\frac{3}{2}}$, $Q_y \propto \sqrt{\Delta}$, to the standard BCS scaling, $Q_i \propto \Delta^2$, where the anisotropy $\delta(T_0, g)$ saturates to a constant.

Quantum fluctuations. Allowing the condensate to flow with momentum $\mathbf{k}_s = (k_x, k_y)$, we expand the free energy at zero temperature in powers of the order parameter ϕ and \mathbf{k}_s . The Ginzburg-Landau (GL) free energy, which fully includes

fluctuation effects, is

$$F_{\text{GL}} = \left(\frac{c_x k_x^2}{\sqrt{mv}} |\phi|^{\frac{3}{2}} + c_y \sqrt{mv} k_y^2 \sqrt{|\phi|} \right) + r(g) \phi^2 + u |\phi|^{\frac{5}{2}}, \quad (15)$$

where $\phi = \Delta + \delta\phi$ gives the order parameter around the saddle-point solution Δ in Eq. (7), $r(g) = (g^{-1} - g_c^{-1})$, $u = \frac{4}{5} c_1 \rho_0$, $c_x = N_0 \Gamma^2(\frac{3}{4}) \Gamma^2(\frac{1}{4}) / 32\pi^3$, and $c_y = N_0 K(\frac{1}{2}) \Gamma^2(\frac{3}{4}) / 16\pi^{\frac{5}{2}}$.

At finite magnetic field, $\mathbf{k}_s = -(2e/\hbar c)\mathbf{A}$ by a suitable gauge choice. Near the QCP, the GL supercurrent $\mathbf{j}_s = c\partial F_{\text{GL}}/\partial\mathbf{A}$ independently recovers Eqs. (11) and (12) at $T = 0$. Hence, the anisotropic quantum critical scaling of the London kernel with ϕ , namely, $Q_y \propto \sqrt{|\phi|}$ and $Q_x \propto |\phi|^{\frac{3}{2}}$, persists near the QCP, where quantum fluctuations dominate.

Because the free energy (15) has nonanalytic terms both in the kinetic energy and in the interaction term u , one cannot expand in the fluctuation fields $\delta\phi$ in order to integrate them out and calculate the quantum fluctuation corrections to the scaling of $\Delta(0, g) \propto (g - g_c)^\beta$, with $\beta = 2$ in mean field [24]. Instead, one needs to resort to field theoretical methods [25,26], which are beyond the scope of this work and will be addressed elsewhere. In any case, the mean-field analysis is accurate in the regime where the quadratic term of (15) dominates over the interaction term u , namely, $(g/g_c - 1)^2 \gtrsim N_0^{-1} v / (\sqrt{m}\Lambda^{\frac{3}{2}})$.

Penetration depth. For a thin film of thickness d , the penetration depth is given by the London kernel, $\lambda_i = \sqrt{-cd/(4\pi Q_i)}$, with $i = x, y$. In general, for systems of semi-Dirac fermions with uniaxial anisotropy, such as in uniaxially strained graphene or semimetallic black phosphorus, the total London kernel is calculated from the Meissner response of a single nodal point times the nodal degeneracy N_0 . In that case, at zero temperature,

$$\lambda_x \propto \frac{\hbar c}{e} \sqrt{d} \Delta^{-\frac{3}{4}}(g) (\sqrt{mv}/N_0)^{\frac{1}{2}}, \quad (16)$$

and

$$\lambda_y \propto \frac{\hbar c}{e} \sqrt{d} \Delta^{-\frac{1}{4}}(g) (\sqrt{mv}N_0)^{\frac{1}{2}}, \quad (17)$$

and hence the penetration depth along the x and y axes grows near the QCP with different scaling exponents, $\lambda_x(g) \propto (1 - g_c/g)^{-3\beta/4}$ and $\lambda_y(g) \propto (1 - g_c/g)^{-\beta/4}$. Near the critical temperature, the penetration depth is still anisotropic, but follows the standard BCS temperature scaling $\lambda \propto \Delta^{-1}(T)$.

Coherence length. In the zero-temperature limit, the coherence length ξ_0 corresponds to the length scale where the energy of the system changes by an amount set by the mass gap 2Δ . Near the neutrality point ($\mu \ll \Delta$, with μ the chemical potential away from half filling), the corresponding change in the momentum domain δp satisfies $\hbar(\delta p) \sim 2\Delta$. Since $\xi_0 \sim \hbar/\delta p$, variations along the direction where the energy spectrum is linear imply that $\xi_{0,y} \sim \hbar v_y/(2\Delta)$. A similar dimensional analysis along the direction of parabolic dispersion gives $\delta p_x \sim \sqrt{2m\Delta}$, and hence

$$\xi_{0,x} \sim \hbar/\sqrt{2m\Delta}, \quad (18)$$

in contrast with the standard Fermi liquid result ($\mu \gg \Delta$), where $\xi_0 \equiv \hbar v_F/(\pi\Delta)$, with v_F the Fermi velocity [17].

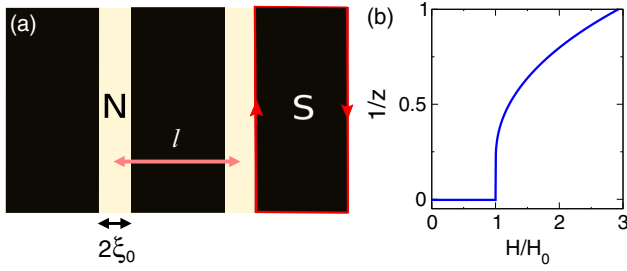


FIG. 4. (a) Stripe phase of superconducting domains (S) oriented along the direction where the order parameter is stiff. The normal regions (N) have a magnetic field H , and width of twice the coherence length ξ_0 . The separation between the center of the stripes is $l \gg \xi_0$. Red lines: Diamagnetic currents. (b) Scaling of $z = l/\lambda$ vs the magnetic field H . For $H \leq H_0 \equiv H_c/\sqrt{\kappa}$, $l \rightarrow \infty$. For $H > H_0$, l is finite.

Fluctuation effects are expected to give small deviations in the quantum critical scaling of the coherence length with Δ due to the emergence of an anomalous dimension.

In mean field, the ratio between the penetration depth in the London limit and the coherence length $\kappa = \lambda/\xi_0$ is given by

$$\kappa_x \sim \Delta^{-\frac{1}{4}}(g)(\sqrt{mv})^{\frac{1}{2}}c \frac{\sqrt{md}}{e}, \quad (19)$$

and

$$\kappa_y \sim \Delta^{\frac{3}{4}}(g)(\sqrt{mv})^{-\frac{1}{2}}\frac{c}{v} \frac{\sqrt{d}}{e}, \quad (20)$$

along the two principal directions x and y , with proportionality factors of the order of 1. Therefore, in the vicinity of the QCP, the order parameter becomes rigid for amplitude variations along the direction where the quasiparticles have linear dispersion [$\kappa_y \propto (1 - g_c/g)^{3/2} \ll 1$], as in type-I superconductors. At the same time, the order parameter becomes soft for variations along the direction of parabolic dispersion [$\kappa_x \propto (1 - g_c/g)^{-1/2} \gg 1$], as in type-II superconductors. While fluctuations could provide corrections to the scaling of κ , the mean-field analysis is suggestive of a possible smectic instability near the QCP.

Stripe phase. The energy of a domain wall becomes negative when $\kappa > 1/\sqrt{2}$. Near the QCP, the magnetic flux can form a stripe pattern of domain walls oriented along the y direction, which coincides with the “easy” direction for the supercurrent, as indicated in Fig. 4(a). Those domains

separate superconducting regions (S), which are screened by diamagnetic currents [red arrows in Fig. 4(a)], from normal regions (N) of width $\sim 2\xi_{0,x}$ separated by a distance $l \gg \xi_{0,x}$. Because the magnetic field H has a stiffness of the order of the penetration depth $\lambda_x \gg \xi_{0,x}$ along the x direction, those domain walls of magnetic flux repel each other and can stabilize a stripe phase in the regime where the magnetic field normal to the sample is strong enough.

Domain wall formation in the bulk of macroscopic samples is elusive and has been observed only in a few ferromagnetic superconductors [27–29]. For samples with finite slab geometry, domain walls are observed in the intermediate state of type I superconductors, where the period of the laminar state is set by the thickness of the sample, $l \propto \sqrt{d}$. In semi-Dirac metals with uniaxial anisotropy, the stripe phase will have a lower energy compared to the vortex state of type-II superconductors near the QCP. In the presence of magnetic fields, the Gibbs free energy of a striped normal domain surrounded by superconducting regions of width l is [30]

$$G(H, z) = \frac{1}{8\pi z} \left(\frac{H_c^2}{\kappa_x} - H^2 \tanh z \right), \quad (21)$$

where $z = l/\lambda_x$ is the distance between the normal domain walls normalized by the penetration depth and H_c is the field that corresponds to the condensation energy $H_c^2/8\pi$. The equilibrium separation between the stripes follows trivially from minimization of the free energy for fixed field, $\partial G(H, z)/\partial z = 0$.

In Fig. 4(b), we show the scaling of $z = l/\lambda_x$ as a function of the magnetic field H . Below the critical field $H < H_c/\sqrt{\kappa_x}$, $l \rightarrow \infty$, and the system has a uniform phase (Meissner state). In the regime $H_c/\sqrt{\kappa_x} < H \lesssim H_c\kappa_x$, l is finite and the system will form a smectic state with stripes of superconducting domains separated by thin strips of magnetic flux. Eventually, when $H \gtrsim H_c\kappa_x$, the separation of the domains $l \sim \xi_{0,x}$ [30] and superconductivity will be destroyed.

Conclusions. In summary, we examined the critical properties of semi-Dirac metal superconductors at zero and finite magnetic fields. We showed that near the quantum critical regime and at finite fields, the anisotropy of the quasiparticles leads to an exotic electromagnetic response which may stabilize a unique smectic state of superconducting stripes.

Acknowledgments. B.U. thanks K. Mullen, M. Fogler, and S. Parmeswaran for helpful discussions. B.U. acknowledges NSF CAREER Grant No. DMR-1352604 for support.

- [1] S. Banerjee, R. R. P. Singh, V. Pardo, and W. E. Pickett, *Phys. Rev. Lett.* **103**, 016402 (2009).
- [2] S. M. Young and C. L. Kane, *Phys. Rev. Lett.* **115**, 126803 (2015).
- [3] H. Huang, Z. Liu, H. Zhang, W. Duan, and D. Vanderbilt, *Phys. Rev. B* **92**, 161115(R) (2015).
- [4] K. Saha, *Phys. Rev. B* **94**, 081103(R) (2016).
- [5] V. Pardo and W. E. Pickett, *Phys. Rev. Lett.* **102**, 166803 (2009).
- [6] G. Montambaux, F. Piechon, J. N. Fuchs, and M. O. Goerbig, *Phys. Rev. B* **80**, 153412 (2009).

- [7] A. S. Rodin, A. Carvalho, and A. H. Castro Neto, *Phys. Rev. Lett.* **112**, 176801 (2014).
- [8] J. Kim *et al.*, *Science* **349**, 723 (2015).
- [9] This state is fundamentally different from multicomponent “type-1.5” superconductivity, where competing coherence lengths lead to phase separation into *vortex* stripes and clusters. See V. Moshchalkov, M. Menghini, T. Nishio, Q. H. Chen, A. V. Silhanek, V. H. Dao, L. F. Chibotaru, N. D. Zhigadlo, and J. Karpinski, *Phys. Rev. Lett.* **102**, 117001 (2009).

- [10] P. Adroguer, D. Carpentier, G. Montambaux, and E. Orignac, *Phys. Rev. B* **93**, 125113 (2016).
- [11] V. N. Kotov, B. Uchoa, V. M. Pereira, F. Guinea, and A. H. Castro Neto, *Rev. Mod. Phys.* **84**, 1067 (2012).
- [12] B. Uchoa and A. H. Castro Neto, *Phys. Rev. Lett.* **98**, 146801 (2007).
- [13] E. Zhao and A. Paramakanti, *Phys. Rev. Lett.* **97**, 230404 (2006).
- [14] Black phosphorus can sustain strain deformations of 30%, which could lead to a comparable reduction in the velocity and enhancement in the mass of the quasiparticles. See Q. Wei and X. Peng, *Appl. Phys. Lett.* **104**, 251915 (2014).
- [15] The normalized specific heat jump is $\delta C_V = \sqrt{2}\gamma_0^2\pi^{3/2}/[\gamma_2(4\sqrt{2}-1)\zeta(\frac{5}{2})] \approx 0.71$, where $\zeta(\frac{5}{2}) \approx 1.34$ is a zeta function, and $\gamma_n \equiv \int_0^\infty dx x^n \sqrt{x} \operatorname{sech}^2 x$, with $\gamma_0 \approx 0.76$ and $\gamma_2 \approx 1.02$.
- [16] B. Uchoa, G. G. Cabrera, and A. H. Castro Neto, *Phys. Rev. B* **71**, 184509 (2005).
- [17] M. Tinkham, *Introduction to Superconductivity* (Dover, New York, 1996).
- [18] See Supplemental Material at <http://link.aps.org/supplemental/10.1103/PhysRevB.96.220503> for [brief description of material].
- [19] A. J. Millis, *Phys. Rev. B* **35**, 151 (1987).
- [20] B. Uchoa and A. H. Castro Neto, *Phys. Rev. Lett.* **102**, 109701 (2009).
- [21] At long wavelengths, virtual plasmons screen the longitudinal component of the supercurrent, maintaining the response of the system invariant under any gauge (see Ref. [22]). For a slab of thickness d , optical plasmons provide screening in the London limit in the presence of any arbitrarily small pocket of charge with energy μ around the nodal points. When $\mu \ll T \ll \Delta$, quantum criticality is reminiscent and drives the critical scaling of the physical observables.
- [22] D. Pines and J. R. Schrieffer, *Nuovo Cimento* **10**, 496 (1958).
- [23] In Hamiltonian (1), the fourfold rotational symmetry of the lattice is restored by the second pair of nodes along the $(1, \bar{1})$ direction of the crystal.
- [24] For Dirac fermions, $\beta = 1$ at the mean-field level and $\beta \approx 0.877$ according to quantum Monte Carlo calculations. See L. Karkkainen, R. Lacaze, P. Lacock, and B. Petersson, *Nucl. Phys. B* **415**, 781 (1994).
- [25] M. Vojta, Y. Zhang, and S. Sachdev, *Int. J. Mod. Phys. B* **14**, 3719 (2000).
- [26] D. V. Khveshchenko and J. Paaske, *Phys. Rev. Lett.* **86**, 4672 (2001).
- [27] R. E. Goldstein, D. P. Jackson, and A. T. Dorsey, *Phys. Rev. Lett.* **76**, 3818 (1996).
- [28] R. Prozorov, *Phys. Rev. Lett.* **98**, 257001 (2007).
- [29] X. Wang, M. Mostovoy, M. G. Han, Y. Horibe, T. Aoki, Y. Zhu, and S.-W. Cheong, *Phys. Rev. Lett.* **112**, 247601 (2014).
- [30] P. G. de Gennes, *Superconductivity of Metals and Alloys* (Addison-Wesley, Boston, 1989).